

High confinement micron-scale silicon nitride high Q ring resonator

Alexander Gondarenko¹, Jacob S. Levy² and Michal Lipson²

1. School of Applied and Engineering Physics, Cornell University, Ithaca, NY, 14853.

2. School of Electrical and Computer Engineering, Cornell University, Ithaca, NY, 14853.
aag42@cornell.edu

Abstract: We demonstrate high confinement, low-loss silicon nitride ring resonators with intrinsic quality factor (Q) of 3×10^6 operating in the telecommunication C-band. We measure the scattering and absorption losses to be below 0.065dB/cm and 0.055dB/cm, respectively.

© 2009 Optical Society of America

OCIS codes: (140.3945) Microcavities; (130.3130) Integrated optics devices; (130.3130) Integrated optics materials

References and links

1. K. Ikeda, R. E. Saperstein, N. Alic, and Y. Fainman, "Thermal and Kerr nonlinear properties of plasma-deposited silicon nitride/ silicon dioxide waveguides," *Opt. Express* **16**(17), 12987–12994 (2008).
2. J. N. Milgram, J. Wojcik, P. Mascher, and A. P. Knights, "Optically pumped Si nanocrystal emitter integrated with low loss silicon nitride waveguides," *Opt. Express* **15**(22), 14679–14688 (2007).
3. S. Gaugiran, S. Gétin, J. Fedeli, G. Colas, A. Fuchs, F. Chatelain, and J. Dérourard, "Optical manipulation of microparticles and cells on silicon nitride waveguides," *Opt. Express* **13**(18), 6956–6963 (2005).
4. A. Serpengüzel, "Amorphous silicon nitride microcavities," *J. Opt. Soc. Am. B* **18**(7), 989–993 (2001).
5. N. Daldosso, M. Melchiorri, F. Riboli, F. Sbrana, L. Pavesi, G. Pucker, C. Kompocholis, M. Crivellari, P. Bellutti, and A. Lui, "Fabrication and optical characterization of thin two-dimensional Si₃N₄ waveguides," *Mater. Sci. Semicond. Process.* **7**(4-6), 453–458 (2004).
6. C. A. Barrios, B. Sánchez, K. B. Gylfason, A. Griol, H. Sohlström, M. Holgado, and R. Casquel, "Demonstration of slot-waveguide structures on silicon nitride / silicon oxide platform," *Opt. Express* **15**(11), 6846–6856 (2007).
7. K. Foubert, L. Lalouat, B. Cluzel, E. Picard, D. Peyrade, E. Delamadeleine, F. de Fornel, and E. Hadji, "Near-field modal microscopy of subwavelength light confinement in multimode silicon slot waveguides," *Appl. Phys. Lett.* **93**(25), 251103 (2008).
8. L. Vivien, D. Marris-Morini, A. Griol, K. B. Gylfason, D. Hill, J. Alvarez, H. Sohlström, J. Hurtado, D. Bouville, and E. Cassan, "Vertical multiple-slot waveguide ring resonators in silicon nitride," *Opt. Express* **16**(22), 17237–17242 (2008).
9. M. Shaw, J. Guo, A. Vawter, S. Habermehl, and C. Sullivan, "Fabrication techniques for low loss silicon nitride waveguides," *Proc. SPIE* **5720**, 109 (2005).
10. J. Guo, M. J. Shaw, G. A. Vawter, P. Esherrick, G. R. Hadley, and C. T. Sullivan, "High-Q integrated on-chip micro-ring resonator," in *Proc. 17th Annu. Meeting IEEE/LEOS*, **2**, pp. 745, (2004).
11. E. Shah Hosseini, S. Yegnanarayanan, M. Soltani, and A. Adibi, "Ultra-High Quality Factor Microdisk Resonators for Chip-Scale Visible Integrated Photonics," in *Frontiers in Optics*, FMG4 (2008).
12. A. Gorin, A. Jaouad, E. Grondin, V. Aimez, and P. Charette, "Fabrication of silicon nitride waveguides for visible-light using PECVD: a study of the effect of plasma frequency on optical properties," *Opt. Express* **16**(18), 13509–13516 (2008).
13. V. R. Almeida, R. R. Panepucci, and M. Lipson, "Nanotaper for compact mode conversion," *Opt. Lett.* **28**(15), 1302–1304 (2003).
14. M. Borselli, T. J. Johnson, and O. Painter, "Accurate measurement of scattering and absorption loss in microphotonic devices," *Opt. Lett.* **32**(20), 2954–2956 (2007).
15. P. Barclay, K. Srinivasan, and O. Painter, "Nonlinear response of silicon photonic crystal microresonators excited via an integrated waveguide and fiber taper," *Opt. Express* **13**(3), 801–820 (2005).

Silicon nitride (Si₃N₄) is a promising material for a waveguide platform due to its low nonlinearity [1] and its transparency in both the visible and infrared spectrum [2–4]. To date silicon nitride waveguides have not been widely employed for propagation at the infrared due to the high tensile stress which limits the thickness of low pressure chemical vapor deposited (LPCVD) Si₃N₄ films to around 250 nm [5–8]. The small film thickness limits the lowest loss modes to quasi-TE (electric field polarized in the substrate plane) which are poorly confined in the nitride and have a very small effective mode index (n_{eff}) < 1.6. Highly delocalized waveguides in the C-band have demonstrated losses as low as 0.1 dB/cm [9] and rings, with diameters as large as several mm, have been shown with quality factors as high as 2.4×10^5 [10]. In the visible spectrum, Adibi *et al.* demonstrated structures with Q 's over 4×10^6 at

wavelength of 655 nm [11]. Plasma enhanced chemical vapor deposition (PECVD) has been recently optimized to deposit Si_xN_y nitride films at low temperature (400°C) with losses below 1 dB/cm at wavelength of 532nm [12].

We demonstrate a method based on temperature cycling and annealing for fabricating low loss Si_3N_4 waveguides with highly confined optical modes. We achieve losses down to 0.12 dB/cm and intrinsic Q 's up to 3,000,000 in single mode ring resonators (Fig. 1). We successfully deposited films up to 744nm in thickness. This thickness, sufficient for the high confinement waveguides used here does not appear to be an absolute limit. A single mode waveguide at this thickness is strongly confined, with an effective index reaching ~ 1.75 for both TE and TM (compared to the bulk material index ~ 2.0).

We fabricate our devices on thermally oxidized silicon wafers. Stoichiometric silicon nitride is deposited in an LPCVD oven at 800°C and 0.1 mTorr. To deposit thick films we cycle the temperature in the deposition process. Layers over 400 nm thick are deposited in multiple steps, allowing wafers to cool to room temperature in between depositions. MaN 2403 e-beam resist is used for patterning with a JEOL 9300 E-beam system. We use a post exposure bake for 5 minutes at 145°C to reflow the resist surface and reduce sidewall roughness. During the reflow the top surface of resist shrinks by $\sim 1\text{-}10\%$ depending on the resist thickness while the bottom surface remains attached to the nitride and does not change size. An inductively coupled plasma reactive ion etcher (ICP RIE), Oxford 100, is used to etch the devices with a CHF_3/O_2 chemistry. Note that etching a 4" wafer with a thickness greater than 400nm requires a pause of the etching process, and the etching of the nitride from the back of the wafer in order to ensure that the thick nitride layer on the backside does not cause excessive stress and break the wafer. Devices are annealed at 1200°C for 20 min in oxygen atmosphere at 1 atm and then in a nitrogen atmosphere for 3 hours. Annealed devices are clad with 460 nm of high temperature silicon dioxide (HTO) deposited at 800°C at 0.2 mTorr. A final silicon dioxide cladding was deposited using a PECVD tool.

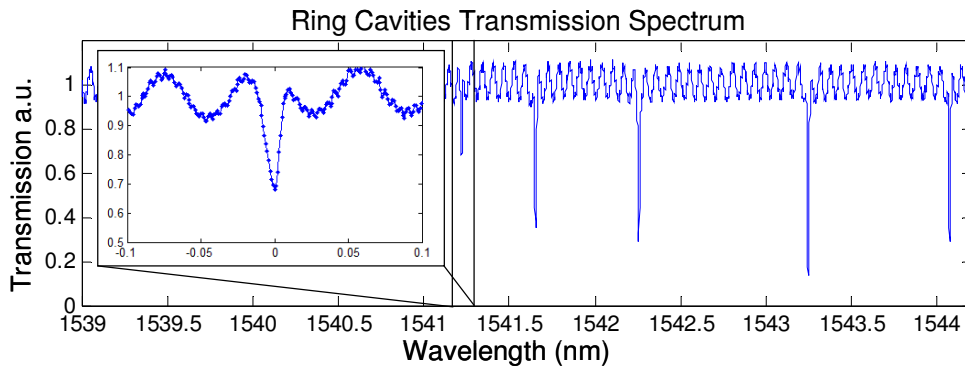


Fig. 1. Transmission spectrum of multiple $40\ \mu\text{m}$ diameter rings coupled to a waveguide. Inset, high resolution spectrum of a 1.5×10^6 coupled Q ring, 5.4×10^6 intrinsic Q , 0.065 dB/cm loss in ring.

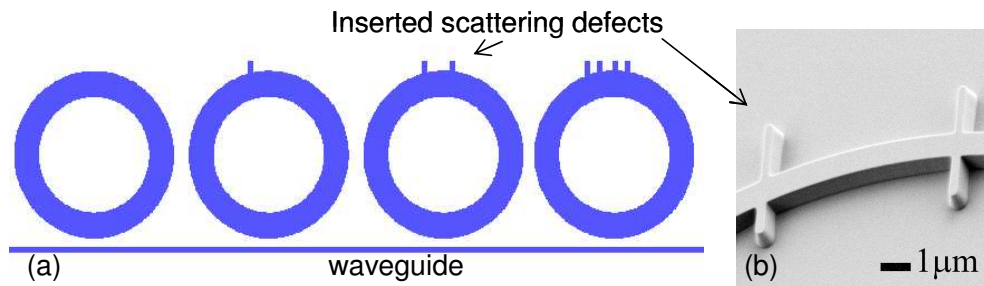


Fig. 2. (a) A series of ring resonators coupled to a single waveguide. The resonators have slightly different radii to distinguish their transmission spectra. (b) SEM micrograph of scattering defects (vertical bars) across a ring resonator inserted to separately measure scattering and absorption losses.

We fabricate multiple ring resonators with radii of ~ 20 μm , height 644 nm, and width of 900 nm coupled to a bus waveguide of the same dimensions. The devices are clad on top and bottom with 4 microns of silicon dioxide. The circumferences of each ring in the series of resonators varies by 80nm to distinguish their resonances. Each ring has from 0 to 8 defects introduced, Fig. 2(b), to increase scattering losses and reduce the Q . The waveguides were terminated with tapers to improve coupling light to fiber [13]. The difference between TE and TM effective indices was ~ 0.03 and minor field component in both polarizations was $< 10\%$ of the major field component. The rectangular cross section was chosen to minimize coupling between the polarizations. The measurement of transmission spectrum of the waveguide coupled rings showed distinct TE and TM resonances with high ($> 20\text{dB}$) extinction for both, ensuring polarization stability.

In order to accurately distinguish between scattering and absorption losses, we introduce carefully engineered defects in the cavities and use Borselli's method [14] to extract linear absorption and scattering coefficients from the optical cavity spectrum. The method consists of measuring the shift of the cavity resonance as a function of the input power coupled into the ring, Fig. 3. The red shift is caused by the temperature increase in the cavity. The temperature change is only dependent on the absorption coefficient (and not on the scattering). The resonance shift as a function of the input power is measured for several rings with different intrinsic quality factors to accurately calculate contributions from different loss mechanisms. The quality factor determines the degree of built up energy in the ring, and therefore the dependence of the resonance shift with the input power.

